Delivery Nanoplatforms Based on Sorafenib and Superparamagnetic Iron Oxide Nanoparticles for Magnetically Targeted Therapy of Hepatocellular Carcinoma

N. Depalo[1], R. M. Iacobazzi[2,3], G. Valente[4], I. Arduino[2], S. Villa[5], F. Canepa[5], V. Laquintana[2], E. Fanizza[4], M. Striccoli[1], A. Cutrignelli[2], A. Lopedota[2], P. Porcelli[3], A. Azzariti[3], M. Franco[2], M. L. Curri[1] and N. Denora[2]

[1] *Istituto per i Processi Chimico-Fisici-CNR UOS Bari, Via Orabona 4, 70125 - Bari, Italy*

[2] *Università degli Studi di Bari Aldo Moro, Dipartimento di Farmacia – Scienze del Farmaco, Via Orabona 4, 70125 - Bari, Italy*

[3] *Istituto Tumori IRCCS Giovanni Paolo II, viale O. Flacco 65, 70124 Bari, Italy*

[4] *Università degli Studi di Bari Aldo Moro, Dipartimento di Chimica, Via Orabona 4, 70125 - Bari, Italy*

[5] *Dipartimento di Chimica e Chimica Industriale, Università di Genova, Via Dodecaneso 31, 16146-Genova, Italy*

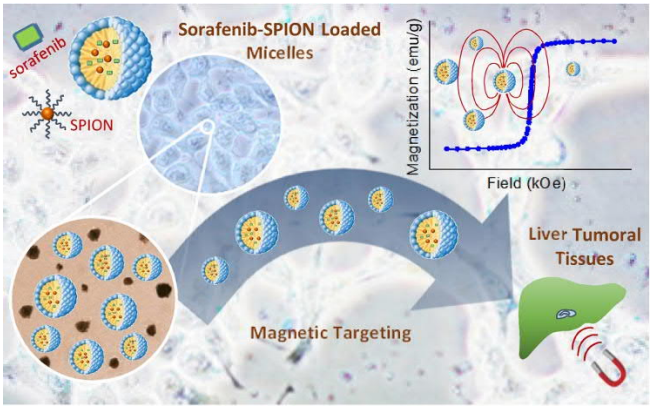

The paper reports on the fabrication of novel magnetic nanoformulations based on polyethylene glycol modified phospholipid micelles loaded with colloidal superparamagnetic iron oxide nanoparticles and sorafenib.

The obtained magnetic nanovectors represent promising candidates for the magnetic targeting of the chemotherapeutic agent to tumor sites towards an efficacious treatment of hepatocellular carcinoma.

Nano Research
DOI (automatically inserted by the publisher)
Review Article/Research Article Please choose one
ISSN 1998-0124
CN 11-5974/O4

Delivery Nanoplatforms Based on Sorafenib and Superparamagnetic Iron Oxide Nanoparticles for Magnetically Targeted Therapy of Hepatocellular Carcinoma

Nicoletta Depalo[1], Rosa Maria Iacobazzi[2,3], Gianpiero Valente[4], Ilaria Arduino[2], Silvia Villa[5], Fabio Canepa[5], Valentino Laquintana[2], Elisabetta Fanizza[4], Marinella Striccoli[1], Annalisa Cutrignelli[2], Angela Lopedota[2], Patrizia Porcelli[3], Amalia Azzariti[3], Massimo Franco[2], Maria Lucia Curri[1] and Nunzio Denora[2] (✉)

[1] *Istituto per i Processi Chimico-Fisici-CNR UOS Bari, Via Orabona 4, 70125 - Bari, Italy,*

[2] *Università degli Studi di Bari Aldo Moro, Dipartimento di Farmacia – Scienze del Farmaco, Via Orabona 4, 70125 - Bari, Italy.*

[3] *Istituto Tumori IRCCS Giovanni Paolo II, viale O. Flacco 65, 70124 Bari, Italy*

[4] *Università degli Studi di Bari Aldo Moro, Dipartimento di Chimica, Via Orabona 4, 70125 - Bari, Italy*

[5] *Dipartimento di Chimica e Chimica Industriale, Università di Genova, Via Dodecaneso 31, 16146- Genova, Italy*

Received: day month year
Revised: day month year
Accepted: day month year (automatically inserted by the publisher)

KEYWORDS

Superparamagnetic Iron Oxide Nanoparticles, PEG-Modified Phospholipid Micelles, Drug delivery, Magnetic targeting, Hepatocellular Carcinoma, Sorafenib

ABSTRACT

Currently, sorafenib is the only systemic therapy capable to increase the overall survival of the patient affected by hepatocellular carcinoma. Unfortunately, its side effects, namely its overall toxicity, limit the therapeutic response that can be achieved. Superparamagnetic iron oxide nanoparticles (SPIONs) are very attractive for drug delivery as they can be targeted to specific sites in the body through the application of a magnetic field, thus improving intracellular accumulation and reducing adverse effects. Here, nanoformulations based on polyethylene glycol modified phospholipid micelles, loaded with both SPIONs and sorafenib, were successfully prepared and thoroughly investigated by means of complementary techniques. The nanovectors resulted effective drug delivery systems with average hydrodynamic diameter of about 125 nm, good stability in aqueous medium and controlled drug loading. Magnetic analysis allowed to determine the correct amount of SPIONs embedded in the micelles. An *in vitro* system was specifically designed to prove that the SPION/Micelles can be efficiently held by using magnetic field under the flow conditions typically found in the human liver. Human hepatocellular carcinoma (HepG2) cells were selected as *in vitro* system to evaluate the tumor cell targeting efficacy of the superparamagnetic micelles loaded with sorafenib. The experiments demonstrated that the delivery platform is able to enhance the drug antitumor effectiveness when magnetically targeted. The herein presented magnetic nanovectors represent promising candidates for the targeting of specific hepatic tumor sites, where the selective release of sorafenib can improve its efficacy and safety profile.

INTRODUCTION

Hepatocellular carcinoma (HCC) is the sixth most common malignancy and the leading cause of mortality in patients with cirrhosis [1]. Curative treatments, such as surgical resection, liver transplantation and local ablation, can improve the survival of HCC patients at an early stage diagnosis. On the contrary, when the tumor is at an advanced stage and a radical surgery is, in most cases, no longer feasible, medical management is the only possible treatment option. Unfortunately, systemic chemotherapy is often limited by drug overall toxicity, and by other mechanisms, such as multiple drug resistance of tumor cells, tumor architecture limiting access of drug to tumor cells, large volume of distribution of drug, resulting in sub-optimal dosing. In contrast to such undesirable results for systemic chemotherapy, there has been a number of encouraging reports on regional and localized chemotherapy. Recent studies have shown increased hepatic uptake of chemotherapeutic agents such as doxorubicin that have led to substantially enhanced response when the agent was administered regionally [2].

Sorafenib, a pan tyrosine kinase receptor inhibitor, is currently the first and sole biological agent clinically approved for patients with advanced HCC [3, 4]. Unfortunately, in some patients (30%) there is no response to the sorafenib therapy and to date the molecular mechanisms responsible of its failure are unknown, even though the microenvironment seems to play a significant role in this issue [5]. Furthermore, the poor aqueous solubility of sorafenib strongly limits its application for local treatment. Therefore, patients with HCC would benefit from the development of a targeted drug delivery system able to concentrate sorafenib at the cancer site, improving its bioavailability, efficacy and safety profile.

Nanoparticle (NP)-based therapeutics offer a new approach to specifically target anticancer drugs to tumor cells and to effectively penetrate resistant cancer cells, thus improving intracellular accumulation and reducing adverse effects of high dose chemotherapy [6-10]. In this perspective, magnetic NPs are very attractive to deliver therapeutics, as they have been reported to be biocompatible, biodegradable and they can be targeted to specific sites in the body through the application of a magnetic field. Magnetic NPs have been extensively studied for their diverse biomedical applications such as Magnetic Resonance Imaging (MRI) contrast agents, hyperthermia, targeted drug delivery, biosensing, and protein separation. So far, several iron oxide NPs have been approved for clinical use [11-13]. In particular, magnetic NP based delivery systems are attractive methods for localizing drug in the body using magnetic forces which act at relatively long range, without affecting most biological tissues [14, 15]. Among them, the superparamagnetic iron oxide nanoparticles (SPIONs) have been widely studied for their use in magnetic fluid hyperthermia but also as drug delivery systems, thus allowing for the multimodal treatment of tumors. Furthermore, SPIONs have been explored for their theranostic potential, as they allow improved contrasting features in MRI. Several clinical trials were performed to validate the safety and the efficacy of these NPs. In this contest, previous experiments clearly showed the improved tumor regression using a combination therapy of SPIONs with doxorubicin [16].

To design and optimize SPION based drug delivery systems, several features need to be considered: (a) the SPIONs should be suitably sized to allow sufficient attraction by the magnetic field and their introduction into the tumor or into the vascular system surrounding the tumor; (b) the magnetic field should be sufficiently intense to attract the magnetic NPs to the desired area; (c) the drug delivery carrier should transport and release a sufficient amount of anticancer agent; and (d) the method of injection should have good access to the tumor vasculature and should avoid a too fast clearance by the reticuloendothelial system.

The design of a drug delivery system requires key features to be accomplished, including size, particle surfaces and coatings, therefore SPION based drug delivery systems need to achieve prolonged blood half-life, improved stability in biological environments and thus increased probability of reaching target cells [17, 18]. NP incorporation in the hydrophobic core of polymer grafted lipid micelles represents an efficient strategy for obtaining nano-formulations with good biocompatibility and

Address correspondence to Nunzio Denora, nunzio.denora@uniba.it

flexibility of the NP surface chemistry [19]. In addition, the approach based on NP encapsulation in lipid micelles allows the further co-incorporation of a wide range of poorly water soluble drugs in the hydrophobic core. Several reports attested the use of micelles as host nanosystem for simultaneous delivery of anticancer drug and magnetic NPs as MRI contrast agent [20-24]. In particular, L. Zhang et al. explored active targeting of sorafenib to human hepatic carcinoma cells using folate functionalized polymeric micelles loaded with SPIONs and sorafenib, thus demonstrating by means of the MRI monitoring system their *in vitro* tumor targeting effect [24]. However, there are still few examples of the use of micelle as nanovectors for active magnetic targeting *via* SPIONs to deliver anticancer drug [25].

Here, micelles based on poly-(ethylene glycol)-phosphoethanolamine (PEG-PE) and loaded with both organic capped SPIONs and sorafenib (SPION/sorafenib/Micelles) have been designed, realized and comprehensively characterized by means of complementary optical, structural and magnetic techniques. PEG-PE is among the most promising polymers, widely used as a carrier for anticancer drug delivery [26-28]. The PEG termination, providing a hydrophilic protective layer at the micelle surface, has demonstrated effective in limiting the natural blood opsonization process of the particles, as it prevents the recognition by macrophages, thus increasing the half-life in blood. Here, for the first time, water dispersible and long term stable lipid based nanoplatforms have been obtained, able to exploit the magnetic targeting of sorafenib to tumor site for an efficacious treatment of the HCC. In order to accomplish such a relevant task, a suitably designed *in vitro* system, simulating the blood flow rates in the liver, has been realized and applied to demonstrate that the SPION loaded micelles can be efficiently held by using clinically acceptable magnetic field [14]. Finally, the *in vitro* tumor cell targeting efficacy of the SPION/sorafenib/Micelles has been evaluated by observing their uptake in human hepatic carcinoma (HepG2) cells, with or without exposure to magnetic field, resulting in an enhanced antitumor effectiveness when magnetically targeted. The future *in vivo* use of the prepared PEG-modified lipid micelles is expected to improve the efficacy safety profile of sorafenib, reducing toxicity and ensuring long circulating time in bloodstreams.

2. EXPERIMENTAL

2.1 Materials

All chemicals were of the highest purity available and were used as received without any further purification or distillation. Oleic acid ($C_{18}H_{33}CO_2H$ or OLEA, 90%), 1-octadecene ($C_{18}H_{36}$ or ODE, 90%), oleyl amine ($C_{17}H_{33}NH_2$ or OLAM, 70%), iron pentacarbonyl ($Fe(CO)_5$, 98%), and dodecan-1,2-diol ($C_{12}H_{24}(OH)_2$ or DDIOL, 90%) and phosphotungstic acid (99.995%) were purchased from Sigma-Aldrich. 1,2-Dipalmitoyl-sn-glycero-3-phosphoethanolamine-*N*-[methoxy (poly(ethylene glycol))-2000] (16:0 PEG-2-PE) was purchased from Avanti Polar Lipids. Sorafenib tosylate was acquired from Selleck Chemicals LLC.

All solvents used were of analytical grade and purchased from Aldrich. All aqueous solutions were prepared by using water obtained from a Milli-Q gradient A-10 system (Millipore, 18.2 MΩcm, organic carbon content $\geqslant$ 4 μg/L). DMEM (Dulbecco's Modified Eagle Medium), FBS (Fetal Bovine Serum), penicillin (100 U/mL) and streptomycin (100 μg/mL) were purchased from EuroClone. Disposable culture flasks and Petri dishes were from Corning (Glassworks). 3-(4,5-Dimethylthiazolyl-2)-2,5-diphenyltetrazolium bromide (MTT) was purchased from Sigma-Aldrich. The magnets were purchased from HKCM Engineering.

2.2 Synthesis of Organic Capped SPIONs

SPIONs were synthesized according to procedures reported in the literature [29, 30]. A mixture containing ODE (20 mL), DDIOL (2.5 mmol), OLAM (3 mmol), and OLEA (3 mmol) was loaded into a three-necked flask connected to a reflux condenser and dried at 110 °C. It was left stirring for 1 h and then heated under N_2 flux to 250 °C. Subsequently, 1 mL of an $Fe(CO)_5$ solution (1 M) in previously degassed ODE was quickly added to the vigorously stirred mixture. The temperature was then lowered to 130 °C, and the reaction mixture was finally cooled to room temperature after exposure to air for 60 min. A solution containing 2-propanol and acetone (1:1 V/V) was added to the mixture, and a black material was precipitated and separated *via* centrifugation (4 cycles). The black product was dissolved in

chloroform to obtain a clear, stable colloidal solution.

2.3 Preparation of SPION/sorafenib/Micelles

Properly adjusted amounts of a SPION stock solution (0.08 M) and sorafenib were co-dissolved in chloroform with 150 µL of 16:0 PEG-2-PE ($3.5 \cdot 10^{-2}$ M). The solvent was rapidly evaporated at 25 °C using a rotary evaporator. The dried SPION/sorafenib/PEG-lipid layer was then kept under vacuum for 1 h. Subsequently, 2 mL of phosphate buffer (PBS, 10 mM, pH 7.4) was added to the film. SPION/sorafenib /Micelles were repeatedly heated to 80 °C (with periodic vigorous mixing) and subsequently cooled to room temperature (three cycles). After micelle formation a centrifuge (5000xg for 1 min) has been carried out to remove the excess of SPIONs or sorafenib which have not eventually embedded in the micelles. Subsequently, since this suspension contained both empty micelles and SPION/sorafenib/Micelles, the empty micelles were removed by ultracentrifugating (200000xg) for 16 hours. The SPION/sorafenib/Micelles formed a pellet while the empty micelles stayed suspended. The supernatant was discarded and the SPION/sorafenib/Micelles were resuspended in water. The solution was filtered by using 0.2 µm filters (Anotop, Whatman) [7, 29, 31] and lyophilized. The dried samples were reconstituted with water or PBS, before their characterization or application. PEG-lipid micelles loaded only with SPIONs (SPION/Micelles) were achieved following the same protocol just without adding the drug.

2.4 Capillary Flow *in Vitro* System

A dynamic circuit used to simulate the blood flow in the liver of human body was appositely designed and realized. Such a circuit was composed of the pipe line formed of a glass capillary tube with the inner diameter of 4 mm and the outer diameter of 6 mm, a mini peristaltic pump (VELP Scientific SP311) operating in the 5-125 ml/min flow rate, a digital fluxmeter (Omega FLR1000 series) to measure the correct flow rate and an in-house built differential pressure sensor to monitor the pressure drop at the end of the accumulation system. A magnetic configuration formed of four NdFeB ring permanent magnets (Magnetic Flux B = 1.27 Tesla), with the inner diameter of 4 mm and the outer diameter of 20 mm, separated by non-magnetic polymeric rings, was set up. The capture of micelles by the permanent magnets configuration was studied by monitoring the variation of Fe (SPIONs) content in the fluid as a function of time. For this purpose, during each 8 hours long experiment, a series of fluid samples was sequentially collected at fixed time and analyzed by ICP-AES (Inductively Coupled Plasma Atomic Emission Spectroscopy).

2.5 Cell Culture

Human liver cancer cells HepG2 were cultured in DMEM high glucose medium supplemented with 10% FBS, 100 U/mL penicillin, 100 µg/mL streptomycin in a humidified incubator at 37 °C with an atmosphere containing 5% of CO_2.

2.6 Cytotoxicity Assays

The cytotoxicity of SPION/sorafenib/Micelles and SPION/Micelles was determinated on human liver cancer cell lines HepG2 using the MTT assay, as described in Denora et al. [32]. Briefly, cells dispensed on 96 microtiter plates at a density of 5,000 cells/well, after overnight incubation, were exposed to SPION/sorafenib/Micelles and SPION/Micelles at six different concentration values, ranging from 0.06 to 300 µg/mL in the nutrient medium. For the SPION/sorafenib/Micelles samples, the tested sorafenib concentration was varied in the range from 0.01 to 50 µM. After 72 h of incubation, an amount of 10 µL of 0.5% w/v MTT was added to each well and the plates were incubated for an additional 3 h at 37 °C. Finally the cells were lysed by addition of 100 µL of DMSO. The absorbance at 570 nm was determined using a PerkinElmer 2030 multilabel reader Victor TM X3. The cell viability of SPION/sorafenib/Micelles was compared with data of the same experiment conducted with pure sorafenib, exploiting sorafenib concentrations varying in the range from 0.01 to 50 µM.

The effect of the magnetic field on cytotoxicity of SPION/Micelles or SPION/sorafenib/Micelles was evaluated as follows: HepG2 cells were seeded in 60 mm tissue culture plates at a density of 500,000 cells/plate and incubated at 37 °C in a humidified atmosphere with 5% CO_2. After 1 day, cells were exposed for 72 h to SPION/Micelles or SPION/sorafenib/Micelles at 60, 30, 6, 0.6 µg/mL in

terms of SPION concentration. For the SPION/sorafenib/Micelles, the tested sorafenib concentrations were 10, 5, 1 and 0.1 μM. The cells were subjected throughout the course of cell incubation to the action of a magnetic field exerted by a NdFeB ring-magnet (outer diameter of 40 mm and an inner diameter of 30 mm, B = 1.17 Tesla). After 72 h of incubation, an amount of 250 μL of 0.5% w/v MTT was added to each well and the plates were incubated for an additional 2 h at 37 °C. Finally, the cells were lysed by addition of 3 mL of DMSO. The absorbance at 570 nm was determined as described above. For comparison, the same experiment was conducted on HepG2 cells incubated with SPION/sorafenib/Micelles without applying any magnetic field.

2.7 Cellular Uptake Study

Cells were seeded in 60 mm tissue culture dishes at a density of 500,000 cells/dish and incubated at 37 °C in a humidified atmosphere with 5% CO_2. After 1 day, the culture medium was replaced with 3 mL of medium containing SPION/Micelles at their IC_{50} concentration (60 μg/mL at 72 h) and incubated for 4 and 24 h with and without application of the magnetic field induced by a NdFeB ring-magnet (outer diameter of 40 mm and an inner diameter of 30 mm, B =1.17 Tesla) or by a NdFeB square-magnet (length 60 mm and width 50 mm, B =1.17 Tesla).

After incubation, the cell monolayer was washed twice with ice-cold PBS and then digested with 2 mL of a HNO_3 (67%)/H_2O_2 (30%), 1:1 (V/V), solution for 4 h at 60 °C in a stove. The iron content was determined by ICP-MS with a Varian 820-MS ICP mass spectrometer.

Uptake of SPION/micelles by the cells was also qualitatively detected using Prussian blue staining. After 4 h of incubation with SPION/Micelles at concentrations of 60 μg/mL in terms of SPION concentration, in absence and in presence of the magnetic field induced by the NdFeB ring-magnet, the HepG2 cells were washed with PBS three times and fixed with 2 mL of 4% paraformaldehyde for 20 minutes. After the repeated washing with PBS, the fixed cells were incubated with 2 mL of Prussian blue solution containing a mixture 1:1 (v/v) of 10% potassium ferrocyanide(II) trihydrate and 10% of hydrochloric acid aqueous solution, at 37 °C for 30 minutes, and then washed with PBS solution three times. Iron staining of the cells was observed under a OLYMPUS CKX41 microscope.

2.8 Cellular Recovery Study

The cell proliferation assay was conducted on HepG2 cells treated with SPION/sorafenib/Micelles (10 μM) and exposed to the magnetic field for 4h (or 24 h) and successive wash out of the medium containing the complex that was replaced with 3 mL of fresh medium. Then, cell viability was assessed after 4, 24, 48 and 72 h and compared with data of the same experiment conducted with sorafenib (10 μM) and SPION/sorafenib/micelles (10 μM in terms of Sorafenib or 60 μg/mL in terms of SPION concentration) without the application of magnetic field.

2.9 Particle Size, Size Distribution and Surface Charge

Hydrodynamic diameter (size), size distribution and colloidal stability of the SPION/Micelles and SPION/sorafenib/Micelles were detected using a Zetasizer Nano ZS, Malvern Instruments Ltd., Worcestershire, UK (DTS 5.00).

In particular, size and size distribution were determined by means of dynamic light scattering (DLS) after sample dilution in demineralized water. Size distribution is described in terms of polydispersity index (PDI). The ζ-potential measurements, *i. e.* the surface charges, were carried out by using a laser doppler velocimetry (LDV) after sample dilution in KCl aqueous solution (1 mM). All reported data are presented as mean values ± standard deviation of three replicates.

2.9 Transmission Electron Microscopy

Transmission Electron Microscopy (TEM) analysis was performed by using a Jeol JEM-1011 microscope, working at an accelerating voltage of 100 kV. TEM images were acquired by an Olympus Quemesa Camera (11 Mpx). The samples were prepared by

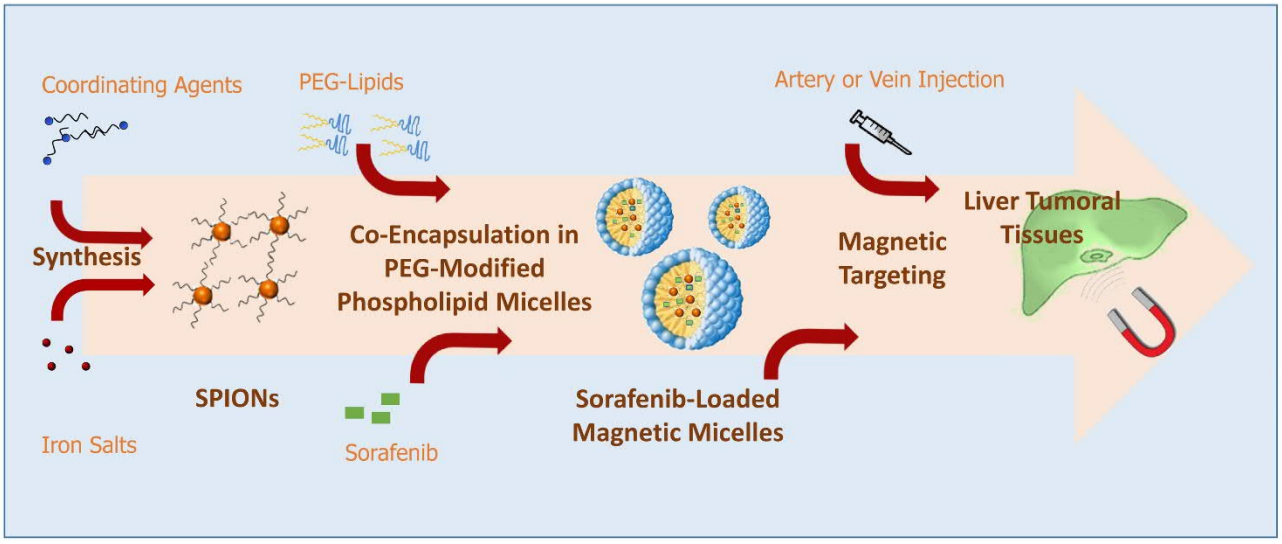

Chart 1. Fabrication route of PEG-modified phospholipid micelles loaded with sorafenib and SPIONs and their possible application for magnetic targeting to liver tumoral tissues

dropping on the 400 mesh amorphous carbon-coated Cu grid a SPION chloroform dispersion or, alternatively, a micelle aqueous suspension, and letting the solvent to evaporate. Size statistical analysis (SPION average size and size distribution) of the samples has been performed by means of a freeware Image J analysis program.

In particular the average NC size and the percentage relative standard deviation ($\sigma_{\%}$) were calculated in order to define the SPION size distribution. For the positive staining TEM observation, after the sample deposition, the grid was dipped in a 2 % (w/v) phosphotungstic acid solution for 30 seconds. Staining agent excess was removed from the grid by rinsing with ultrapure water (dipping the grid in ultrapure water three times for 10 seconds). The sample on the grid was left to dry overnight and finally stored in a vacuum chamber until analysis. For the negative staining TEM investigation, 30 µL of a 2 % (w/v) phosphotungstic acid solution were cast on the grid where the sample had previously been deposited. Staining agent excess was removed by blotting, at the edge of the grid, with filter paper, wetted with ultrapure water. After complete drying of the sample, the grid was stored in a vacuum chamber until analysis.

2.10 Magnetic Measurements

AC magnetic susceptibility measurements were performed by using an OXFORD Maglab2000 system operating in the 1–10^4 Hz frequency range with an AC magnetic field of 10 Oe. The resolution of the AC signal was higher than 10^{-7} emu. Room temperature DC magnetization measurements were carried out by means of a commercial DC-SQUID magnetometer (MPMS Quantum Design) with a resolution higher than 10^{-8} emu (RSO option).

2.11 HPLC-UV Analysis

HPLC-UV investigation was performed by using an Agilent 1260 Infinity Quaternary LC System equipped with a UV-VIS 1260 Infinity Multiple Wavelength Detector and a Rheodyne Manual Sample Injector Valves 7725i. Sorafenib was separated on Zorbax Eclipse Plus C18 column (4.6 x 250 mm, 5 mm). The system was operated isocratically using a mobile phase consisting of a mixture of Milli-Q water and methanol at a ratio of 20:80 V/V and pumped at a flow rate of 1 mL/min at 25°C. The UV detector was set at a detection wavelength of 250 nm.

3. RESULTS AND DISCUSSION

In this work, PEG-modified phospholipid micelles loaded with organic capped SPIONs and sorafenib are proposed as nanovectors, potentially able to efficiently and selectively deliver the chemotherapeutic for the treatment of HCC to the tumor sites, by using magnetizable implants. In order

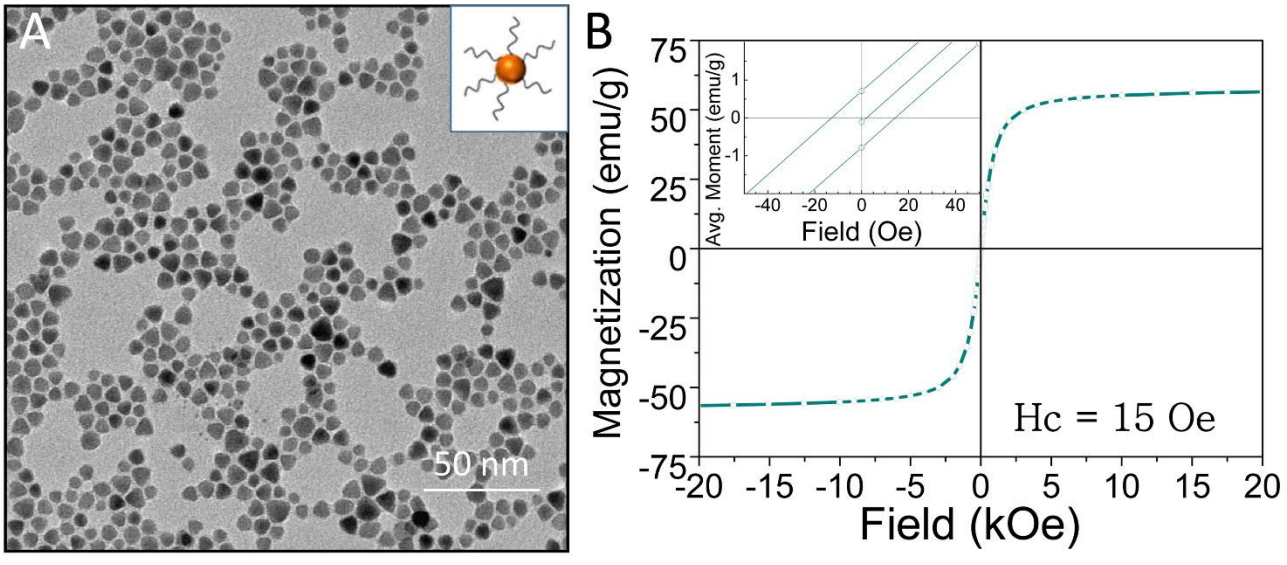

Figure 1. TEM micrograph (A) and RT hysteresis cycle (B) of organically capped SPIONs

to accomplish such relevant tasks the nanostructure size and surface charge stability, as well as SPION and antitumor drug loading, have needed to be carefully tailored to achieve a nanoformulation with high colloidal stability in physiological medium and ability to be attracted by the magnetic field and penetrate into the tumor or into the vascular system surrounding the tumor, where the drug cargo should be released. Starting from such assumptions, SPION/sorafenib/Micelles were here successfully prepared by exploiting the hydrophobic nature of surface SPIONs and, at the same time, the very poor water solubility (~10-20 μM) of the antitumor drug. Chart 1 reports the route to achieve the fabrication of the magnetic and therapeutic nanoformulation for potential application.

3.1 Synthesis and Characterization of Organic Capped SPIONs

The "*as prepared*" organic capped SPIONs, synthesized by following the experimental procedure reported by Buonsanti et al., have been characterized by TEM measurements, as well as, SQUID analysis [30].

The TEM micrograph reported in Figure 1A clearly shows SPIONs exhibiting a quite regular spherical or triangular shape, with a mean diameter of (8.8 ± 0.9) nm (Figure 1A). The powder X-ray diffraction pattern of SPIONs reported by Buonsanti et al. can be ascribed to the cubic spinel structure of both γ-Fe_2O_3 (maghemite) and Fe_3O_4 (magnetite), as well as to a mixture of both phases, thus preventing their discrimination due, also, to the significant line broadening [30]. In fact, the interference fringe pattern for the SPIONs revealed by high-resolution TEM images was compatible with both maghemite and magnetite phases [29].

Magnetic properties of "*as synthesized*" SPIONs were evaluated by a SQUID magnetometer. In particular, SQUID measurements, carried out at room temperature, confirmed the complete superparamagnetic character of the SPIONs. The data indicated that magnetic properties of SPIONs are amenable for their use in biomedical applications, since SPIONs mainly demonstrated magnetic behavior only in the presence of an applied external magnetic field.

A high saturation magnetization value (Ms = 56.5 emu/g) has been observed for this organically coated SPIONs. RT bulk magnetization values of SPIONs are 90 emu/g and 74 emu/g for Fe_3O_4 and γ-Fe_2O_3, respectively. However, reduced magnetization values are commonly observed in magnetite and maghemite NPs, due to the spin canting of magnetic moments at the NP surface [33]. Furthermore, RT saturation

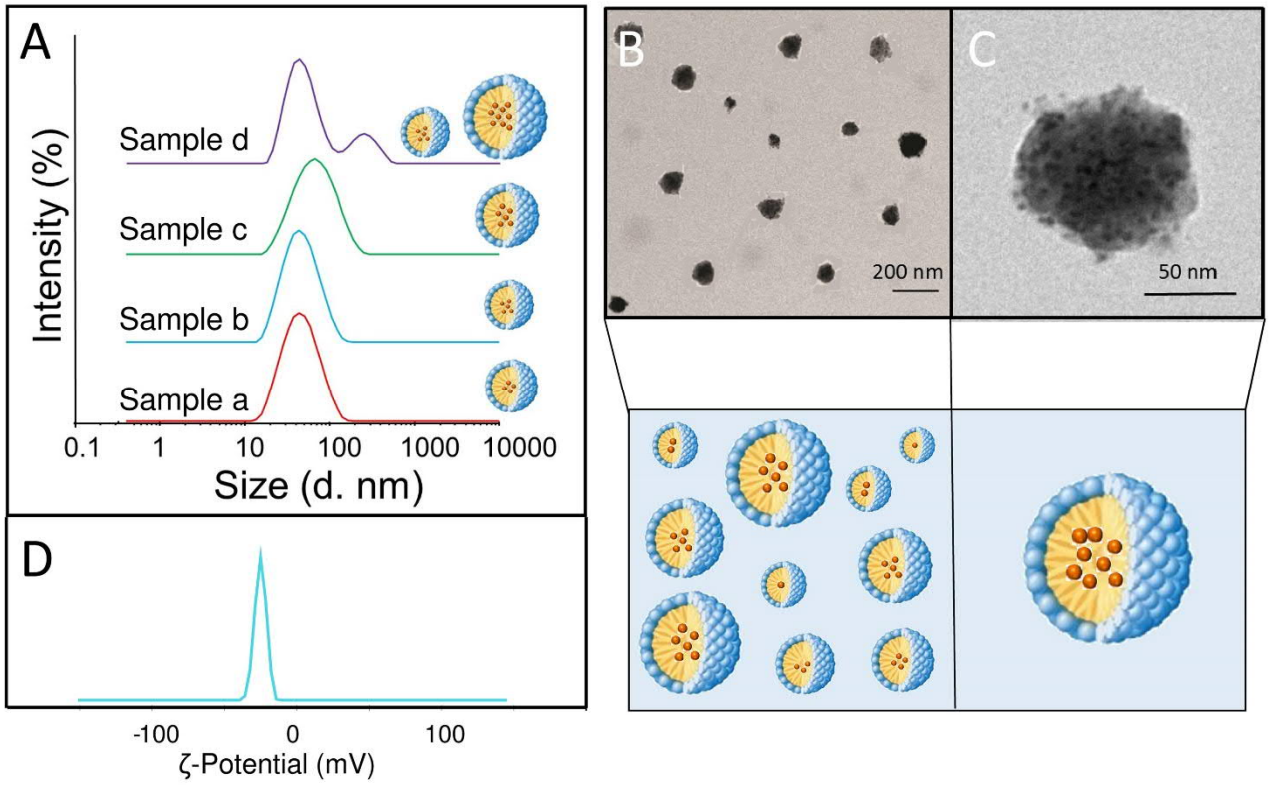

Figure 2. Size distribution obtained by DLS of the SPION/Micelles samples prepared starting from SPION weight percentage of 16% (a), 20% (b), 24% (c) e 28% (d) (A). TEM micrographs obtained with positive (B) and negative (C) staining, respectively, for the 20% weight SPION sample (b) dispersed in aqueous PBS buffer along with their corresponding sketches of SPIONs encapsulated in the hydrophobic core of PEG-PE micelles. ζ-potential measurement of the same sample dispersed in PBS buffer (D).

magnetization values are also affected by NP dimensions [34]. Since experimental values range from 60.5 [35] to 70 emu/g [36] for magnetite and from 32 [37] up to 53 emu/g [38] for maghemite types of NPs, respectively, the experimental magnetization value found here, 56.5 emu/g, does not allow to discriminate between the two crystal structures of iron oxide magnetic NPs.

3.2 Preparation and Characterization of SPION/Micelles

Preliminary studies have been performed on the SPION/Micelles at increasing SPION content, in order to investigate the effect of the magnetic cargo on hydrodynamic size and size distribution of the micelles. Furthermore, the colloidal stability in physiological media of the SPION based nanovectors, as well as, their actual effective magnetic behavior upon application of a suitable extracorporeal magnet have been thoroughly investigated. The SPION/Micelles have been prepared at fixed PEG-PE concentration value and varying the SPION weight percentage. Namely, four samples have been prepared at a starting SPION weight percentage of 16 (a), 20 (b), 24 (c) and 28% (d), respectively. A morphological and structural investigation of the SPION/Micelles has been performed by means of DLS and TEM analysis. DLS analysis revealed a monomodal size distribution for the samples a, b and c, providing hydrodynamic diameter of 48 (PDI=0.193±0.015), 50 (PDI=0.181±0.007), and 63 nm

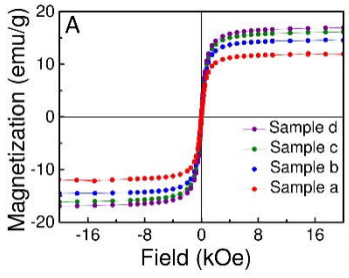

B

	M_s (emu/g)	Actual SPION Weight (%)
SPIONs	56.5 ± 0.5	100
Sample a	11.9 ± 0.1	21
Sample b	14.5 ± 0.1	26
Sample c	16.2 ± 0.2	28
Sample d	17.0 ± 0.2	30

Figure 3. RT Hysteresis cycles of SPION/Micelles at increasing SPION load. Namely starting SPION content is 16 (a), 20 (b), 24 (c) and 28 (d) weight %, respectively (A). Actual SPION content in % weight in the four different SPION/Micelles samples as calculated from RT saturation magnetization (Ms) values (B).

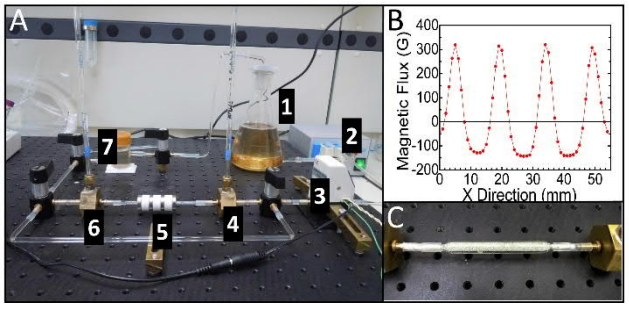

Figure 4 Picture of the dynamic circuit with (1) accumulation vessel, (2) peristaltic pump, (3) digital flowmeter, (4,6) in-house built differential pressure sensors, (5) magnetic accumulation system, (7) sampling holder (A). Gradient of the magnetic field along the flow direction (X Direction) (B). Organic tissue simulation before the circulation of the magnetic fluid (C).

(PDI=0.217±0.016), respectively (Figure 2 A, red, blue and green line, respectively). Conversely, DLS investigation performed on sample d has resulted in a bimodal size distribution, indicating that smaller aggregates coexist with larger aggregates (Figure 2A, violet line). In particular, average hydrodynamic diameters of 51 and 212 nm have been recorded for the smaller and larger aggregates, respectively (PDI=0.379±0.049). Therefore, high monodispersity and homogeneity have been observed for sample a, b and c, while the formation of larger aggregates observed in the sample d, occurred owing to the high starting SPION concentration. The average hydrodynamic diameter values recorded for the overall samples suggest the formation of micellar aggregates containing a variable number of SPIONs clustered in a single micelle. Such an assumption is definitely supported by the TEM investigation. TEM micrographs, with positive and negative staining, of sample b, which, from the DLS analysis, resulted to be the most monodisperse samples among the investigated ones, highlighted the formation of PEG-PE micelles each containing not just one SPION, but rather aggregates formed of more SPIONs, ranging from 30 to 100 nm (Figure 2 B and C).

The results of the ζ-potential measurements indicated the overall high colloidal stability of the samples, resulting in a ζ-potential value of (–25 ± 1) mV (Figure 2 D). Furthermore, the PEG hydrophilic chains exposed at the surface of micelles is expected to convey the micelles a steric stabilization, in addition to the electrostatic one, bringing stealth properties to the system.

SQUID measurements, carried out at room temperature, confirmed the complete superparamagnetic character of the SPIONs after their incorporation in the micelles, thus proving that their encapsulation allows to retain their superparamagnetic properties. This result is particularly amenable for the future *in vivo* applications, since the micelles loaded with SPIONs can be magnetically driven, without, however, exhibit any residual magnetic interaction at body temperature, and ultimately prevent, or anyway significantly limiting, their agglomeration. Indeed, such a feature allows, in principle, the prepared SPION/Micelles to remain circulating after injection and crossing through the capillary systems of organs and tissues avoiding vessel embolism and thrombosis. Interestingly, RT dynamic magnetic measurements as a function of the frequency (data not reported), confirmed the results achieved by TEM and DLS analysis. A numerical fit, based on the previously reported magnetic model [39], resulted, indeed, in a mean diameter of the SPION/Micelles in solution around 80 nm. Furthermore, the RT magnetic hysteresis cycles, shown in Figure 3 A, performed on the four different (a, b, c and d) samples, have been compared with the results on bare SPIONs (Figure 1 B) and allowed to promptly calculate the actual

amount of SPIONs embedded in the different samples of PEG-micelles. The results on such calculations based on the SQUID measurements on the different sample of SPION/Micelles are summarized in Figure 3 B. The SPION content as a weight % values obtained by magnetic measurements and reported in Table B (Figure 3) appear in fact higher than those theoretically calculated as a ratio between the starting SPION weight and the total sample weight (16, 20, 24 and 28%). Such a result can be reasonably explain taking into account that the ultracentrifugation cycles performed on the samples after the micelle formation eliminate the empty micelles which remain dispersed in the supernatant (see Experimental Section). Therefore, the overall lipid content, and consequently the total weight of the samples decreases, resulting in an actual SPION weight % higher than that theoretically estimated in the starting samples. Interestingly, the magnetic investigation demonstrated an extremely effective and not destructive tool to rapidly and carefully assess the actual amount of SPIONs in the lipid based nanoformulations.

3.3 Magnetic Targeting Simulations in a Capillary Flow *in Vitro* System

A key issue in magnetic delivery is represented by the ability of the SPIONs to remain effectively confined in target regions of the body against blood flow which tends to carry them away. Therefore, the behavior of the SPION/Micelles has been investigated by using an *in vitro* system, purposely designed to simulate the flow rate of the blood stream in the liver. In particular, a dynamic circuit composed of an accumulation vessel, peristaltic pump, digital flowmeter, homemade differential pressure sensor, magnetic accumulation system and sampling holder has been specifically developed (Figure 4). In such an accumulation system, a magnetic NP, in a dynamic fluid, under a fixed flow rate and a static magnetic field, experiences an attractive magnetic force defined as

$$F_M = V_{NP} \cdot \chi_{NP} \cdot H(x) \cdot \left(\frac{\partial H}{\partial z}\right)_x$$

where V_{NP} is the volume of the NP, χ_{NP} is the magnetic susceptibility (correlated with the magnetization) of the NP, H(x) is the magnetic field at x distance from the magnet and $(\partial H/\partial z)x$ is the gradient of the magnetic field in the flow direction.

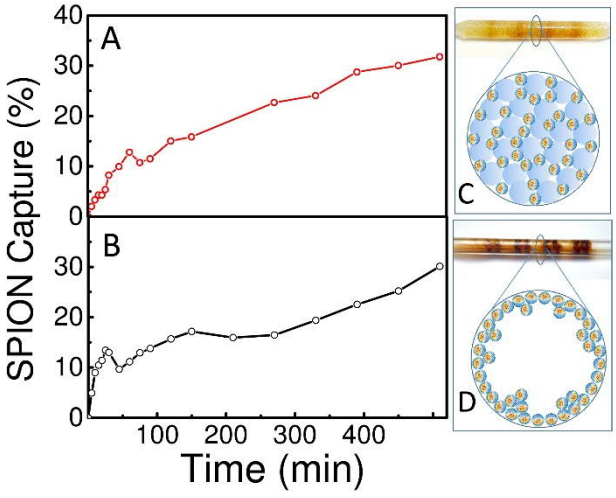

Figure 5 Amount (as a percent of the initial content) of captured SPION/Micelles in an organic tissue simulation (A) and in the capillary flow model (B) system, respectively. Picture of glass capillary filled with glass spheres (C) and of glass empty capillary (D) along with their corresponding schematic sketch after circulation of the solution containing SPION/Micelles and removal of the NdFeB ring magnets.

It is, therefore, evident that for a large magnetic force acting on a NP, a great value of the product $H(x)\cdot(\partial H/\partial z)_x$ is required. Since the flow is perpendicular to the magnetic force, the flow rate will interfere with the attractive force of the magnet, *i. e.* higher flow rates will correspond to a decreased number of magnetic nanocarriers captured by the magnetic field. Hence, a magnetic configuration formed by four NdFeB ring permanent magnets with inner diameter of 4 mm and outer diameter of 20 mm separated by non-magnetic polymeric rings has been designed and used. Such a configuration allows to increase the number of capture zones inside the capillary glass (Figure 5B) introduced in the rings, *i.e.* the number of zones where the $H(x)\cdot(\partial H/\partial z)_x$ product is maximum.

The SPION/Micelles (sample b) have been dispersed in a physiological solution at pH 7.4 at a concentration of 80 mg/L. The speed capture of the defined NdFeB ring magnets (B=1.27 Tesla) configuration has been tested at two different flow rates, namely 100 and 50 mL/min, for the circulation of the solution in the

capillary flow model system. After eight hours, an amount corresponding to 28% of the initial magnetic micelles have been found to be captured under a 50 mL/min flow rate, as assessed by means of ICP-AES analysis (Figure 5B). Such a value as been observed to slightly decrease down to 23% at the highest investigated flow rate of 100 mL/min, as reasonably expected (data not reported). The proposed *in vitro* model has been clearly designed only to mimic the most basic features of blood vessels since there are numerous additional factors that could influence magnetic targeting, including as the mechanical and surface properties of the blood vessel wall. Therefore, since the *in vivo* flow of micelles in liver should be surely affected by many obstacles in the form of cells and extracellular matrix components, a second model system including, instead, a larger, glass tube (8 mm inner diameter) completely filled with glass spheres with diameters ranging from 0.8 up to 1 mm (void fraction around 0.5) has been proposed and used to simulate an organic tissue (Figure 4 C). A flow rate of 50 mL/min, has been identified as optimal for the investigated dynamic configuration under the specific conditions. A similar configuration of four NdFeB ring permanent magnets has served for the micelle dynamic circulation. In this case (Figure 5A), a height hours accumulation resulted in 32 % of micelles capture, as calculated on the basis of the results of the ICP-AES elemental analysis. The recorded enhancement in the capture rate can be reasonably related to the increased resistance of the SPION/Micelles due to the friction with the surface of the glass spheres in the channel, that, affecting the flow rate inside the accumulation vessel, further assists the magnetic capture. These experiments have highlighted, firstly the effect of the flow rate on the SPION/Micelles capture degree and, in addition the increase of the capture in the more realistic "simulated" organic tissue.

3.4 Preparation and Characterization of SPION/sorafenib/Micelles

The subsequent step of the work has been represented by the co-encapsulation of both the SPIONs and sorafenib within the hydrophobic micellar core.

In particular, the effect of drug feeding on encapsulation efficiency has been investigated, being such a parameter defined as the amount (w/w %) of sorafenib encapsulated with respect to the starting amount used in the preparation of nanoformulation. The amount of drug caught in the micelles has been quantified by HPLC analysis.

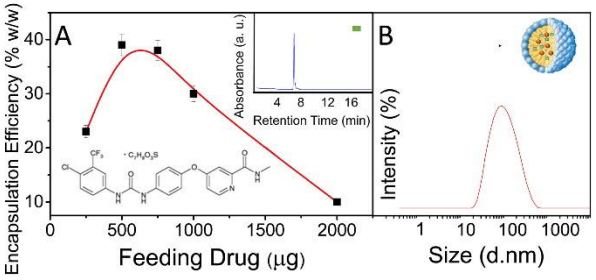

Figure 6 Encapsulation drug efficiency in the PEG-PE micelles as function of sorafenib feeding calculated by HPLC analysis (A). HPLC chromatogram obtained from pure sorafenib by UV absorption at 250 nm (Inset A). Size distribution obtained by DLS of SPION/sorafenib/Micelles prepared starting from initial 20% SPION weight and 1 mg of sorafenib (B).

Initially, in the micelle preparation an increase in the initial amount of sorafenib at fixed starting SPION weight (20%), lead to an increase of the amount of drug encapsulated, as quantified by encapsulation efficiency values (Figure 6). The obtained results suggested that, although the encapsulation load efficiency reaches the maximum value (40%) when the feeding drug is 500 μg, with an actual loading of 150μM, the highest actual loading (235 μM) in the resulting nanoformulation was observed at a starting sorafenib feed of 1 mg.

When the initial amount of drug is higher than 1 mg, however, the amount of macroscopic precipitation occurring during micelle preparation also increases. Consequently, this macroscopic precipitation has also contributed to decrease the loading. DLS analysis has revealed a homogeneous and monomodal size distribution of SPION/sorafenib/Micelles, resulting in an average hydrodynamic diameter of 125 nm (PDI=0.370±0.025).

In addition, ζ-potential value of (-25± 2) mV resulted in accordance with the value obtained for SPION/Micelles, therefore proving the effective sorafenib incorporation with SPIONs in the hydrophobic core of micelles and highlighting again

the high colloidal stability of micelles in aqueous solution, essential requirement to perform the *in vitro* and *in vivo* experiments.

3.5 *In Vitro* Cytotoxicity Assay

The cytotoxic effects of the SPION/sorafenib/Micelles on the viability of human hepatic carcinoma cell line, namely HepG2, has been assessed by performing an *in vitro* toxicity study after a long-term exposure of cells, and has been finally evaluated by the MTT assay.

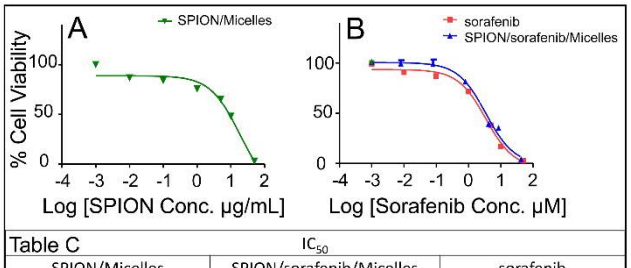

Table C	IC_{50}	
SPION/Micelles (μg/mL)	SPION/sorafenib/Micelles (μM)	sorafenib (μM)
58.8 ± 0.2	3.20 ± 0.06	2.63 ± 0.03

Figure 7 Viability results for HepG2 cells after incubation for 72 h with SPION/Micelles (A) or SPION/sorafenib/Micelles (B, blue line) or pure sorafenib (B, red line), respectively. IC_{50} values, resulting from the same viability assays, expressed as SPION concentration for SPION/Micelles and as sorafenib concentration for SPION/sorafenib/Micelles and pure sorafenib. Data presented as mean ± standard error of the three distinct experiments performed in triplicate (Table C).

The ability of free sorafenib to interfere with the cell viability has been also estimated using untreated cells as control. In addition, the effect of the SPION/Micelles on cell viability has been preliminary assessed, in order to rule out the SPION/Micelles cytotoxicity contribution from the cytotoxicity specifically ascribable to the anticancer drug loaded in SPION/sorafenib/Micelles (Figure 7). In particular, HepG2 cells have been incubated for 72 h with SPION/Micelles at SPION concentration values ranging from 300 to 0.06 μg/mL (Figure 7 A). The recorded IC_{50} value is (58.8 ± 0.2) μg/mL in terms of SPION concentration (Figure 7, Table C). The cytotoxicity study has indicated that the viability of the HepG2 cells is only minimally affected after 72 h of incubation with sorafenib-free micelles. Conversely, cytotoxicity study performed on SPION/sorafenib/Micelles under the same experimental conditions tested for SPION/Micelles (72 h, with SPION concentration ranging from 300 to 0.06 μg/mL) and sorafenib concentration values ranging from 50 to 0.01 μM, has revealed an enhanced and drug concentration dependent cytotoxic effects on HepG2 cells (Figure 7 B, blue line).

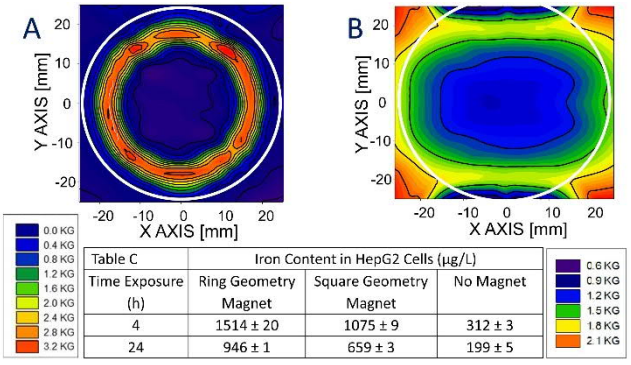

Table C	Iron Content in HepG2 Cells (μg/L)		
Time Exposure (h)	Ring Geometry Magnet	Square Geometry Magnet	No Magnet
4	1514 ± 20	1075 ± 9	312 ± 3
24	946 ± 1	659 ± 3	199 ± 5

Figure 8 Graphical representation of the magnetic flux maps utilized for the uptake HepG2 liver cell evaluation of the SPION/Micelles and generated using a ring magnet (A) and square magnet (B). Iron content determined by ICP-MS analysis in HepG2 liver cancer cells after their incubation for 4 h and 24 h, with SPION/Micelles without application of magnetic field and under exposure to a ring or square magnet (Table C).

In particular, the IC_{50} values, expressed as a function of sorafenib concentration, is (3.20 ± 0.06) μM at a SPION concentration of 22.38 μg/mL (Figure 7, Table C). Therefore, the toxic effect of SPION/sorafenib/Micelles on cell viability can be mainly ascribed to the presence of chemotherapeutic agent in the nanoformulation, since the cytotoxicity study performed on SPION/Micelles has indicated that the SPION concentration of 22.38 μg/mL not affected at all the viability of HepG2. Consistently, the IC_{50} values recorded for SPION/sorafenib/Micelles has resulted quite comparable to those obtained by incubation of HepG2 cells with pure sorafenib for 72 h, namely (2.63 ± 0.03) μM (Figure 7 B, red line and Table C). This first set of experimental results has thus highlighted that the antitumor activity of sorafenib is still fully preserved once embedded in the

hydrophobic micelle cores.

3.6 Effect of Magnetic Targeting on Cellular Uptake of SPION/Micelles

Preliminarly to the assessment of the effect of the cell exposure to magnetic field on cell viability and cellular uptake of SPION/sorafenib/Micelles, two distinct NdFeB magnets with the same magnetic induction value (B =1.17 Tesla) but with different shape have been tested in order to identify the most suitable magnet geometry to ensure the highest cellular uptake. In particular, a ring and a square shaped magnet, respectively, with the magnetic field maps shown in Figure 8 A and B, have been, alternatively, positioned externally at the bottom of the Petri dish. Cells treated under the same experimental conditions, containing the HepG2 cells incubated with SPION/Micelles, at SPION concentration of 60 μg/mL, for 4 and 24 h, without exposure to magnetic field have been used as reference, while the control has been represented by untreated cells. The cellular uptake of SPION/Micelles, occurring with and without cell exposure to the field of the two different magnets, has been evaluated as iron content by means ICP-MS analysis. The data reported in Table C of Figure 8 clearly show that the exposure to magnetic field has strongly increased the SPION/Micelle uptake in HepG2 cells at both the two explored incubation time. In addition, the ring-magnet has resulted to possess the most suitable geometry to promote a more efficient internalization of SPION/Micelle in HepG2 cells, already after 4 h incubation. The evidence of the SPION/Micelle intracellular uptake in HepG2 cells has been qualitatively evaluated by using Prussian Blue staining and optical microscopy. The *in vitro* study has been carried out by incubating the HepG2 cells with SPION/Micelles at SPION concentration of 60 μg/mL for 4 h, exposed or not to the magnetic field, generated by the ring shaped magnet, which has been demonstrated more effective to inducing an enhanced cellular uptake than the squared magnet. The Prussian blue staining experiments. shown in Figure 9, point out that the degree of cellular uptake of the SPION/Micelles is strongly depended on the presence of magnetic field. In particular, the cells show a much more intense blue staining when incubated with the SPION/Micelles and exposed to the magnetic field (Figure 9 B), whereas the blue spots in the cells treated with the SPION/Micelles under the same conditions have been found significantly less intense in absence of magnetic field (Figure 9 A).

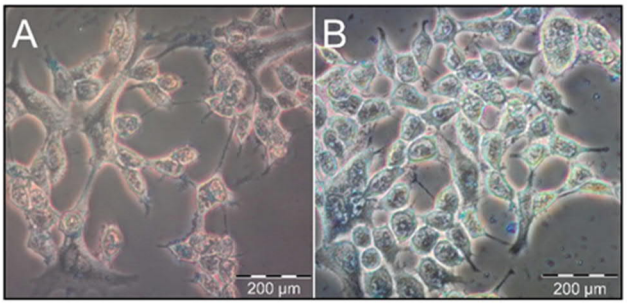

Figure 9 Prussian blue staining images for HepG2 liver cells after 4 h incubation with SPION/Micelles (SPION concentration of 60μg/mL) without (A) and with (B) exposure of ring geometry magnet.

Such a test has been able to further qualitatively prove how the magnetic targeting is able to promote an enhanced cellular uptake, confirming the quantitative results obtained by ICP analysis (Figure 8, Table C). A decline in the intracellular iron concentration has been in any case observed at treatment for 24 h (Figure 8, Table C). This decrease can be reasonably ascribed to the fact that, after 24 h of cell incubation with SPION/Micelles, a certain extent of cell death can occur, thus suggesting an inherent cytotoxic effect of the tested formulation. In fact, the uptake study has been carried out at a SPION concentration of 60 μg/mL, that is the IC_{50} value obtained for the cells treated with SPION/Micelles at 72 h. In addition, the cytotoxicity study, performed on HepG2 cells treated with SPION/Micelles, at SPION concentration ranging from 0.6 to 60 μg/mL for 72 h, with and without cell exposure to magnetic field, indicates that the presence of magnetic field did not induce an enhancement in the toxicity on the cell treated with SPION/Micelles (Figure 10 A), being the cell viability values recorded

for cells exposed to the magnetic field comparable to those unexposed. Therefore, while the presence of magnetic field promotes an enhanced cell internalization of SPION/Micelles, still the cell viability remains unaffected. The decrease of the cell viability observed after 72 h at SPION concentration of 60 µg/mL (Figure 10 A) suggests that cell viability also decline already at 24 h, thus causing a partial loss of the SPIONs accumulated in the dead cells and ultimately resulting in a final iron content lower than that one found after 4 hours (Figure 8).

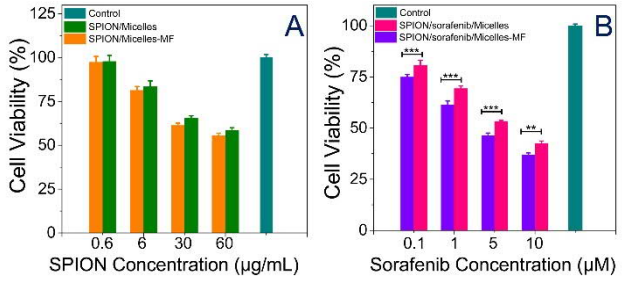

Figure 10 Cell viability of HepG2 cells after 72 of incubation with Micelle-SPION targeted by a magnetic field or not targeted. (A) % Cell viability of HepG2 cells after incubation with SPION/Sorafenib/micelles (0.1-10 µM in terms of sorafenib concentration and 0.06 to 60 µg/mL in terms of SPION) in presence and absence of a magnetic field. Each compound has been tested in triplicate, and the experiments were repeated three times. Statistical significance has been calculated using a two-way analysis of variance (ANOVA) followed by the Bonferroni post hoc tests (GraphPad Prism vers. 5). *= $p<0.05$, ** $p<0.01$, *** $p<0.001$ (B).

The observed decline of cell viability in a SPION concentration-dependent way can be reasonably explained assuming that, after their cellular internalization, SPION/Micelles can release the originally contained SPIONs. Therein, they lose iron ions, that can induce oxidative stress via generation of reactive oxygen species (ROS), through energy or electron transfer to molecular oxygen [27, 40]. Clearly, the effect on cell viability has been found further enhanced at the highest tested SPION concentrations.

3.7 Effect of Magnetic Targeting on the Antitumor Efficacy of SPION/sorafenib/Micelles

The antitumor efficiency of sorafenib, when delivered by means magnetic targeting and incorporated in the micellar system, has been investigated by evaluating the cell viability after incubation of HepG2 cells for 72 h with the SPION/sorafenib/micelles in presence of magnetic field. Sorafenib concentration value ranging from to 0.1 to 10 µM, at a corresponding SPION concentration varying from 0.06 to 60 µg/mL, have been thus investigated.

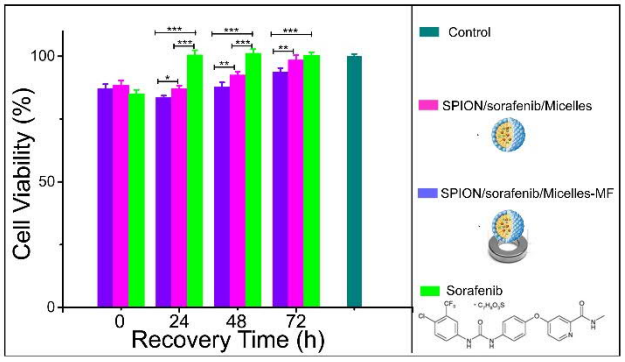

Figure 11 Cell viability of HepG2 cells measured after incubation for 4 h with different formulation 10 µM in sorafenib and 60 µg/mL in SPIONs, both exposed or unexposed to the magnetic field (MF).

As a control, untreated cells have been used. Results reported in Figure 10 B show that the SPION/sorafenib/Micelles have affected the cell viability in a concentration dependent manner, and viability values obtained for the cells exposed to the magnetic field have resulted slightly lower than those recorded for the cells treated with SPION/sorafenib/Micelles but unexposed to the magnetic field. As already demonstrated, the cell viability of SPION/micelles, tested under the same experimental conditions, is comparable whether recorded in presence or not of the magnetic field, although exposure to the magnetic field induces an enhanced intracellular uptake.

Therefore, the drug co-encapsulated with SPIONs in the micelles can be considered responsible of the cytotoxicity, recorded under the same experimental conditions for the cell treated with SPION/sorafenib/Micelles and exposed to the magnetic field, that has been found higher than those observed for the cells incubated but unexposed to the magnetic field.

The enhanced intracellular uptake of

SPION/sorafenib/Micelles, due to cell exposure to magnetic field, has a significant impact, as it allows accumulation of higher sorafenib dose in the cells, thus promoting an improved antitumor effect of the drug when magnetically targeted and delivered by means the here explored magnetic lipid nanovectors.

Finally, the major antitumor efficacy of the magnetically targeted SPION/sorafenib/Micelles respect to native free drug has been investigated by incubating the HepG2 cells with SPION/sorafenib/micelles at a sorafenib concentration of 10 μM (SPION concentration 60 μg/mL) for 4 h whether exposed or not to the ring shaped magnet induced field. Subsequently, the medium containing the micelles has been replaced with a fresh medium. In the case of cells treated and exposed to the magnetic field, the ring magnet has been removed after the incubation of 4 hours with SPION/sorafenib/micelles. Following the removal of the micelles containing medium, the cells have been let to recover for 24, 48 and 72 h, respectively, before testing possible effects of the drug and assessing cell viability. The cells treated with the native free sorafenib have been used as reference, under the same experimental conditions (Figure 11). Immediately after the cell incubation with the SPION/sorafenib/micelles (exposed or unexposed to the magnetic field) or the free sorafenib for 4 h, the cell viability results have been found comparable to those recorded at time 0. This evidence, that is the lack of any detectable difference in the cell death induced by drug encapsulated in the magnetic lipid nanocarriers with respect to that induced by free sorafenib, can be reasonably accounted for by a slow release kinetics of SPION/sorafenib/Micelles, as also established by Fang et al. for C6-ADR cells treated with SPIONs loaded with doxorubicine [41]. Interestingly, once free drug has been removed and the cells have been incubated with fresh medium for 24 h, the cells recovered and grew as prior to the drug exposure. Conversely, the SPION/sorafenib/Micelles treated cells have shown cell viability values, recorded after SPION/sorafenib/Micelles removal and 24 h of cell incubation with pure culture medium, of (83.5 ± 0.8)% and (87.1 ± 2.2)%, for the cells exposed and unexposed to the magnetic field.

The lower cell viability observed for cells treated with SPION/sorafenib/Micelles exposed respect to those unexposed to the magnetic field can be safely ascribed to the higher intracellular uptake of the micelles containing SPIONs when magnetically targeted in the cells (Figure 11). After 48 h by incubation with pure culture medium, the cells treated with SPION/sorafenib/Micelles have begun to recover and grow. The cell recovery process has resulted evident after 72 h. This behavior suggests that the sorafenib release profile of SPION/sorafenib/Micelles is able to maintain an intracellular drug concentration longer than the free sorafenib and that their magnetically targeted uptake allows a more efficient internalization of SPION/sorafenib/Micelles in cells, thus promoting an enhanced cytotoxic effects, ultimately achieving an antitumor efficiency significantly higher than that presented by the free drug.

This latter observation has been confirmed by a further recovery cell experiment, carried out by incubating the HepG2 cells with SPION/sorafenib/micelles at sorafenib concentration of 10 μM for 24 h, either exposed or not to the magnetic field and by assessing cell viability 72 h after the removal of the micelles. As expected, the cell viability values have been found lower for cell treated with SPION/sorafenib/Micelles exposed to the magnetic field than for the unexposed, namely of (72.5 ± 2.1)% vs (80.2 ± 1.5)%, thus further highlighting the enhanced antitumor activity of the prepared nanoformulations by magnetic targeting.

4. CONCLUSIONS

Nanoformulations based on PEG-modified lipid micelles loaded with SPIONs and sorafenib have been designed and realized by exploiting a simple and reproducible strategy that has allowed to obtain magnetic nanovectors characterized by a significantly high stability in aqueous medium and a careful control on the drug loading. The magnetic characterization has not only confirmed the successfully encapsulation of SPIONs in the core of the micelles, but, remarkably, has also demonstrated an extremely effective tool to determine the actual amount of magnetic NPs in the formulation. The design and the application of the *in vitro* dynamic circuit simulating the blood flow rates in the liver has definitely proven that the SPION/Micelles could be efficiently held by using magnetic field, thus resulting potentially able to be magnetically targeted to tumor

sites under the flow conditions typically found in the human liver.

A systematic study on the *in vitro* response of HepG2 cells exposed to SPION/sorafenib/Micelles provided relevant insight on their toxicity, whether exposed or unexposed to the magnetic field. The cytotoxicity of free sorafenib has been also evaluated, along with the effect of SPION/Micelles on cell viability, to investigate on the possible different factors specifically affecting cell viability. The experimental results have demonstrated that the antitumor activity of sorafenib is still fully preserved upon encapsulation in the hydrophobic micelle cores and that the presence of magnetic field promotes an enhanced cell internalization of SPION/Micelles, without, however, affecting the cell viability. Finally, cell recovery experiments have highlighted the occurrence of release kinetics slower in the case of the SPION/sorafenib/Micelles than in the free sorafenib incubated cells.

Remarkably a superior antitumor effectiveness of the magnetically targeted SPION/sorafenib/Micelles has been found. The obtained PEG-PE micelles have enabled the convenient combination of the drug with magnetic NP based nanovectors in one versatile nanoformulation that can be suitably driven towards tumor tissues, envisioning a high impact on magnetically targeted therapy of HCC.

Acknowledgements

The University of Bari (Italy) and the Inter-University Consortium for Research on the Chemistry of Metal Ions in Biological Systems (C.I.R.C.M.S.B.) are gratefully acknowledge for their financial support. The work has been also supported by Nanomax-integrable sensors for pathological biomarkers diagnosis (N-CHEM) and NANOfotocatalizzatori per un'Atmosfera più PULita (NANOAPULIA) projects.

References

[1] Villanueva, A.; Llovet, J. M. Targeted Therapies for Hepatocellular Carcinoma. *Gastroenterology*. **2011**, 140, 1410–1426.

[2] Goodwin, S. C.; Bittner, C. A.; Peterson, C. L.; Wong, G. Single-Dose Toxicity Study of Hepatic Intra-arterial Infusion of Doxorubicin Coupled to a Novel Magnetically Targeted Drug Carrier. *Toxicol. Sci*. **2001**, 60, 177-183.

[3] Deng, G. L.; Zeng, S.; Shen, H. Chemotherapy and target therapy for hepatocellular carcinoma: New advances and challenges. *World J. Hepatol*. **2015**, 7, 787–798.

[4] El-Serag, H. B.; Marrero, J. A.; Rudolph, L.; Reddy, K. R. Diagnosis and treatment of hepatocellular carcinoma. *Gastroenterology*. **2008**, 134, 1752-1763.

[5] Azzariti, A.; Porcelli, L.; Quatrale, A. E.; Paradiso, A.; Giannelli, G. Sorafenib effectiveness is inhibited in presence of Laminin-5 in HCC Cells. *Journal of Hepatology*. **2012**, 56, S71–S224.

[6] Kumar, A.; Jena, P. K.; Behera, S.; Lockey, R. F.; Mohapatra, S.; Mohapatra, S. Multifunctional magnetic nanoparticles for targeted delivery. *Nanomedicine: Nanotechnology, Biology and Medicine*. **2010**, 6, 64–69.

[7] Valente, G.; Depalo, N.; de Paola, I.; Iacobazzi, R. M.; Denora, N.; Laquintana V.; Comparelli, R.; Altamura, E.; Latronico, T.; Altomare, M.; Fanizza, E.; Striccoli, M.; Agostiano, A.; Saviano, M.; Del Gatto, A.; Zaccaro, L.; Curri, M. L. Integrin-targeting with peptide-bioconjugated semiconductor-magnetic nanocrystalline heterostructures. *Nano Research*. **2016**, 9, 644–662.

[8] Fanizza, E.; Iacobazzi, R. M.; Laquintana, V.; Valente, G.; Caliandro, G.; Striccoli, M.; Agostiano, A.; Cutrignelli, A.; Lopedota, A.; Curri, M. L.; Franco, M.; Depalo, N.; Denora, N. Highly selective luminescent nanostructures for mitochondrial imaging and targeting. *Nanoscale*. **2016**, 8, 3350-3361.

[9] Laquintana, V.; Denora, N.; Lopalco, A.; Lopedota, A.; Cutrignelli, A.; Lasorsa, F. M.; Agostino, G.; Franco, M. Translocator protein ligand-plga conjugated nanoparticles for 5-fluorouracil delivery to glioma cancer cells. *Mol. Pharm.* **2014**, 11, 859-871.

[10] Denora, N.; Cassano, T.; Laquintana, V.; Lopalco, A.; Trapani, A.; Cimmino, C.S.; Laconca, L.; Giuffrida, A.; Trapani, G. Novel codrugs with GABAergic activity for dopamine delivery in the brain. *Int. J. Pharm.* **2012**, 437, 221-231.

[11] Prijic, S.; Sersa, G. Magnetic nanoparticles as targeted delivery systems in oncology. *Radiol. Oncol*. **2011**, 45, 1-16.

[12] Arruebo, M.; Fernández-Pacheco, R.; Ibarra, M. R.; Santamaría, J. Magnetic nanoparticles for drug delivery. *Nanotoday*. **2007**, 2, 22-32.

[13] Veiseh, O.; Gunn, J.; Zhang, M. Design and fabrication of magnetic nanoparticles for targeted drug delivery and imaging. *Adv. Drug Deliv. Rev*. **2010**, 62, 284–304.

[14] Owen, J.; Rademeyer, P.; Chung, D.; Cheng, Q.; Holroyd, D.; Coussios, C.; Friend, P.; Pankhurst, Q. A.; Stride, E. Magnetic targeting of microbubbles against physiologically relevant flow conditions. *Interface Focus*. **2016**, 6, 20150097.

[15] Alexiou, C.; Arnold, W.; Klein, R. J.; Parak, F. G.; Hulin, P.; Bergemann, C.; Erhardt, W.; Wagenpfeil, S.; Lubbe, A. S. Locoregional Cancer Treatment with Magnetic Drug Targeting. *Cancer Research*. **2000**, 60, 6641–6648.

[16] Liang, P. C.; Chen, Y. C.; Chiang, C. F.; Mo, L. R.; Wei, S. Y.; Hsieh, W. Y.; Lin, W. L. Doxorubicin-modified magnetic nanoparticles as a drug delivery system for magnetic resonance imaging-monitoring magnet-enhancing tumor chemotherapy. *International Journal of Nanomedicine*. **2016**, 11, 2021–2037.

[17] Veiseh, O.; Gunn, J. W.; Zhang, M. Design and fabrication of magnetic nanoparticles for targeted drug delivery and imaging. *Adv. Drug Deliv. Rev*. **2010**, 62,284-304.

[18] Shapiro, B.; Kulkarni, S.; Nacev, A.; Muro, S.; Stepanov, P. Y.; Weinberg, I. N. Open challenges in magnetic drug targeting. *WIREs Nanomed Nanobiotechnol*. **2015**, 7, 446–457.

[19] Kamaly, N.; Xiao, Z.; Valencia, P. M.; Radovic-Moreno, A. F.; Farokhzad, O. C. Targeted polymeric therapeutic nanoparticles: design, development and clinical translation. *Chem. Soc. Rev*. **2012**, 41, 2971–3010.

[20] Ao, L.; Wang, B.; Liu, P.; Huang, L.; Yue, C.; Gao, D.; Wu,

C.; Su,W. A folate-integrated magnetic polymer micelle for MRI and dual targeted drug delivery. *Nanoscale*. **2014**, 6, 10710–10716.
[21] Ye, F.; Barrefelt, A.;, Asem, H.;, Abedi-Valugerdi, M.; El-Serafi, I.;, Saghafian, M.; Abu-Salah, K.; Alrokayan, S.; Muhammed, M.; Hassan, M. Biodegradable polymeric vesicles containing magnetic nanoparticles, quantum dots and anticancer drugs for drug delivery and imaging. *Biomaterials*. **2014**, 35, 3885-3894.
[22] Hu, J.; Qian, Y.; Wang, X.; Liu, T.; Liu, S. Drug-Loaded and Superparamagnetic Iron Oxide Nanoparticle Surface-Embedded Amphiphilic Block Copolymer Micelles for
Integrated Chemotherapeutic Drug Delivery and MR Imaging. *Langmuir*. **2012**, 28, 2073-2082.
[23] Pouponneau, P.; Leroux, J.-C.; Soulez, G.; Gaboury, L.; Martel, S. *Biomaterials*. **2011**, 32, 3481-3486.
[24] Zhang, L.; Gong, F.; Zhang, F.; Ma, J.; Zhang, P.; Shen, J. Targeted therapy for human hepatic carcinoma cells using folate-functionalized polymeric micelles loaded with superparamagnetic iron oxide and sorafenib in vitro. *International Journal of Nanomedicine*. **2013**, 8, 1517-1524.
[25] Lin, M. M.; Kang, Y. J.; Sohn, Y.; Kim, D. K. Co-encapsulation of magnetic nanoparticles and doxorubicin into biodegradable microcarriers for deep tissue targeting by vascular MRI navigation. *J. Nanopart. Res.* 2015, 17, 248.
[26] Wang, J.; Wang, Y.; Liang, W. Delivery of drugs to cell membranes by encapsulation in PEG–PE micelles. *J. Control. Release*. **2012**, 160, 637–651.
[27] Wang, J.; Fang, X.; Liang, W. Pegylated Phospholipid Micelles Induce Endoplasmic Reticulum-Dependent Apoptosis of Cancer Cells but not Normal Cells. *ACS Nano*. **2012**, 6, 5018-5030.
[28] Wang, Y.; Wang, R.; Lu, X.; Lu, W.; Zhang, C.; Liang, W. Pegylated Phospholipids-Based Self-Assembly with Water-Soluble Drugs. *Pharm. Res.* **2010**, 27, 361-370.
[29] Depalo, N.; Carrieri, P.; Comparelli, R.; Striccoli, M.; Agostiano, A.; Bertinetti, L.; Innocenti, C.; Sangregorio, C.; Curri, M. L. Bio-functionalization of anisotropic nanocrystalline semiconductor-magnetic heterostructures. *Langmuir.* **2011**; 27,6962-6970.
[30] Buonsanti, R.; Grillo, V.; Carlino, E.; Giannini, C.; Curri, M. L.; Innocenti, C.; Sangregorio, C.; Achterhold, K.; Parak, F. G.; Agostiano, A.; Cozzoli, P. D. Seeded growth of asymmetric binary nanocrystals made of a semiconductor TiO_2 rodlike section and a magnetic gamma-Fe_2O_3 spherical domain. *J. Am. Chem. Soc.* **2006**, 128, 16953-16970.
[31] Depalo, N.; Mallardi, A.; Comparelli, R.; Striccoli, M.; Agostiano, A.; Curri, M. L. Luminescent nanocrystals in phospholipid micelles for bioconjugation: An optical and structural investigation. *J. Colloid. Interface Sci*. 2008, 325, 558-566.
[32] Denora, N.; Laquintana, V.; Lopalco, A.; Iacobazzi, R. M.; Lopedota, A.; Cutrignelli, A.; Iacobellis, G.; Annese, C.; Cascione, M.; Leporatti, S.; Franco, M. In vitro targeting and imaging the translocator protein TSPO 18-kDa through G(4)-PAMAM–FITC labeled dendrimer. *J. Control. Release*. **2013**, 172, 1111-1125.
[33] Coey J. M. D. Non collinear spin arrangement in ultrafine ferromagnetic crystallites. *Physical Review Letters.* **1971**, 27, 1140-1142.
[34] Kolhaktar, A.G.; Jamison, A. C.; Litvinov, D.; Willson, R. C.; Lee T. R. Tuning the magnetic properties of nanoparticles. *Int. J. Mol. Sci.* **2013**, 14, 15977-16009.
[35] Zhang, Y.-Q.; Wei, X.-W.; Yu, R. Fe_3O_4 Nanoparticles-Supported Palladium-Bipyridine Complex: Effective Catalyst for Suzuki Coupling Reaction. *Catal. Lett.* **2010**, 135, 256–262.
[36] Riani P.; Napoletano M.; Canepa F., Synthesis, characterization and a.c. magnetic analysis of magnetite nanoparticles. *J. Nanopart. Res.* **2011**, 13, 7013-7020.
[37] Nurdin, I.; Johan, M. R.; Yaacob, I. I.; Ang, B. C.; Andriyana, A. Synthesis, characterization and stability of superparamagnetic maghemite nanoparticle suspension. Materials Research Innovations. **2014**, 18, S6-203.
[38] Kluchove, K.; Zboril, R.; Tucek, J.; Pecova, M.; Zajoncova, L.; Safarik, I.; Mashlan, M.; Markova, I.; Jancik, D.; Sebela, M.; Bartonkova, H.; Bellesi, V.; Novak, P.; Petridis, D. Superparamagnetic maghemite nanoparticles from solid-state synthesis – Their functionalization towards peroral MRI contrast agent and magnetic carrier for trypsin immobilization. *Biomaterials*. **2009**, 30, 2855-2863.
[39] Riani, P.; Lucchini, M. A.; Thea, S.; Alloisio,, M.; Bertoni, G.; Canepa, F. New Approach for the Step by Step Control of Magnetic Nanostructure Functionalization. *Inorg. Chem.* **2014**, 53, 9166–9173.
[40] Latronico, T.; Depalo, N.; Valente, G.; Fanizza, E.; Laquintana, V.; Denora, N.; Fasano, A.; Striccoli, M.; Colella, M.; Agostiano, A.; Curri, M. L.; Liuzzi, G. M. Cytotoxicity Study on Luminescent Nanocrystals Containing Phospholipid Micelles in Primary Cultures of Rat Astrocytes. *PLoS ONE*. **2016**, 11, e0153451
[41] Fang, C.; Kievit, F. M.; Veiseh, O.; Stephen, Z. R.; Wang, T.; Lee, D.; Ellenbogen, R. G.; Zhang, M. Fabrication of Magnetic Nanoparticles with Controllable Drug Loading and Release through a Simple Assembly Approach. *J. Control. Release*. **2012**, 162, 233–241.